# Mechanistic Insights into Ring-Closing Enyne Metathesis with the Second-Generation Grubbs-Hoveyda Catalyst: A DFT Study

**ARTICLE** *in* CHEMISTRY - A EUROPEAN JOURNAL · JUNE 2011

Impact Factor: 5.73 · DOI: 10.1002/chem.201003410 · Source: PubMed



**5 AUTHORS**, INCLUDING:

Francisco Nuñez-Zarur
University of Antioquia
**18** PUBLICATIONS **175** CITATIONS
SEE PROFILE

Xavier Solans-Monfort
Autonomous University of Barcelona
**47** PUBLICATIONS **1,232** CITATIONS
SEE PROFILE

Luis Rodríguez-Santiago
Autonomous University of Barcelona
**73** PUBLICATIONS **1,666** CITATIONS
SEE PROFILE

Mariona Sodupe
Autonomous University of Barcelona
**189** PUBLICATIONS **4,590** CITATIONS
SEE PROFILE

CHEMISTRY
A EUROPEAN JOURNAL

DOI: 10.1002/chem.201003410

# Mechanistic Insights into Ring-Closing Enyne Metathesis with the Second-Generation Grubbs–Hoveyda Catalyst: A DFT Study

**Francisco Nuñez-Zarur, Xavier Solans-Monfort,* Luis Rodríguez-Santiago, Roser Pleixats, and Mariona Sodupe[a]**

**Abstract:** The full catalytic process (precatalyst activation, propagating cycle and active-species interconversion) of the ring-closing enyne metathesis (RCEYM) reaction of 1-allyloxy-2-propyne with the Grubbs–Hoveyda complex as catalyst was studied by B3LYP density functional theory. Both the ene-then-yne and yne-then-ene pathways are considered and, for the productive catalytic cycle, the feasibility of the *endo*-yne-then-ene route is also explored. Calculations predict that the ene-then-yne and yne-then-ene pathways proceed through equivalent steps, the only major difference being the order in which they take place. In this way, all alkene metathesis processes studied here involve four steps: olefin coordination, cycloaddition, cycloreversion and olefin decoordination. Among them, the two more energetically demanding ones are the olefin coordination and decoordination steps. The reaction of the alkyne fragment consists of two steps: alkyne coordination and alkyne skeletal reorganization, the latter of which has the highest Gibbs energy barrier. Comparison between the ene-then-yne and yne-then-ene pathways shows that there is no clear energetic preference for either of the two processes, and thus both should be operative when unsubstituted enynes are involved. In addition, although the *endo* orientation is computed to be slightly disfavored, it is not ruled out for 1-allyloxy-2-propyne, and thus calculations seem to indicate that the *exo* versus *endo* selectivity is strongly influenced by the presence of substituents in the reagent.

**Keywords:** density functional calculations · enynes · metathesis · reaction mechanisms · ruthenium

## Introduction

The term "olefin metathesis" was first used in 1967 by Calderon and co-workers when referring to the skeletal reorganization reaction of two double bonds.[1] Since then great efforts have been made, and nowadays olefin metathesis has become one of the most powerful tools in organic synthesis, because it allows the formation of new carbon–carbon double bonds even in the presence of functional groups.[2–5] Advances in olefin metathesis and particularly in the development of new catalysts[3] have made it applicable in many useful processes in academia and industry, such as cross-metathesis (CR), ring-closing metathesis (RCM), ring-opening olefin metathesis polymerization (ROMP), and enyne metathesis.[6–9] In particular, enyne metathesis, first reported by Katz and Sivavec in 1985,[10] refers to the skeletal reorganization of a double bond with a triple bond leading to a conjugated diene (Scheme 1).[6,8,9] Two main subtypes of enyne metathesis can be distinguished: 1) intramolecular (ring-closing enyne metathesis, RCEYM) leading to formation of cyclic products (Scheme 1a)[11,12] and 2) intermolecular, with an acyclic diene as final product, which was first reported by Blechert and co-workers[13] (Scheme 1b).

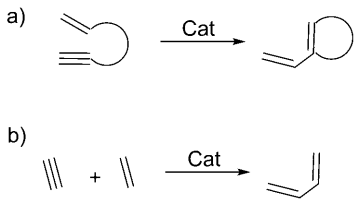


Scheme 1.

Despite the great knowledge achieved in olefin metathesis (mechanism, catalyst development, product selectivity),[2,3] less is known about the enyne reaction, for which several points still remain unclear. For instance, two different mechanisms have been postulated.[6,9,14–20] It has been proposed that the reaction takes place by an ene-then-yne mechanism, as shown in Scheme 2a. This pathway implies first the reaction between the double bond and the metal carbene.[16] Alternatively, some experimental evidence suggests that the alkyne can be the first to react with the metal alkylidene, leading to the yne-then-ene mechanism (Scheme 2b and c).[15,20] Noteworthily, several recent works have suggested that the two processes may occur simultaneously and that

[a] Dipl. Chem. C. F. Nuñez-Zarur, Dr. X. Solans-Monfort, Dr. L. Rodríguez-Santiago, Prof. R. Pleixats, Prof. M. Sodupe
Departament de Quimica
Universitat Autònoma de Barcelona
08193 Bellaterra, Cerdanyola del Vallès (Spain)
Tel: (+34) 935812173
E-mail: xavi@qf.uab.es

Supporting information for this article is available on the WWW under http://dx.doi.org/10.1002/chem.201003410.

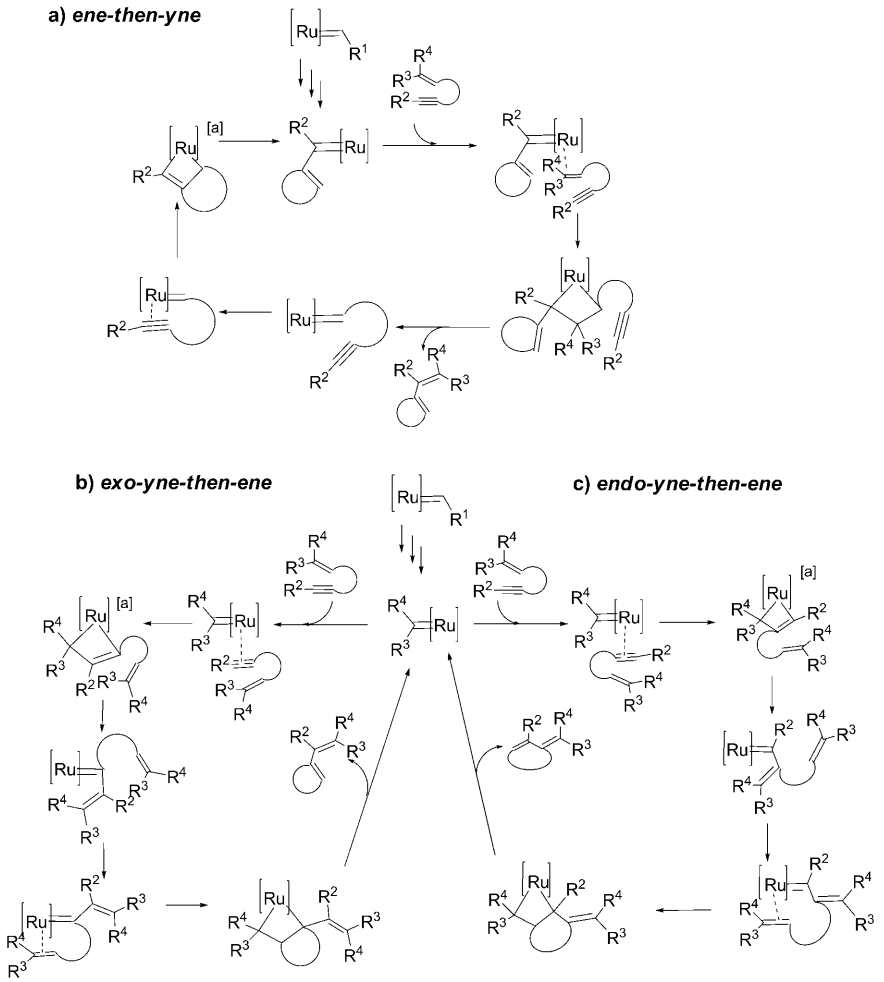


Scheme 2. [a] Metallacyclobutene intermediates are not minima of the potential energy surface.

the preferred route depends on several factors such as the catalyst, the reactants and the reaction conditions.[6,17–19,21] This catalytic process is even more complex, since two different pathways can be distinguished for the yne-then-ene mechanism depending on the substrate orientation, that is, the *exo* (Scheme 2b) and the *endo* (Scheme 2c) approaches, which in general lead to different products.[6,9,17,18] However, even if formation of the *endo* product seems plausible, it is usually not observed when an Ru-based catalyst is used, or it is only observed in minor amounts.[6,17,18,20] In fact, to our knowledge the number of examples in which the *endo* product is the major one is very small.[18]

Many theoretical studies have dealt with Ru-based metathesis reactions[22,23] but, to our knowledge, only three studies have considered the enyne case[21,24,25] and only two[21,24] of them the intramolecular process. They agree that, although alkyne coordination to the metal is preferred, ene-then-yne seems to be the most favourable pathway. Nevertheless, different conclusions are obtained regarding how large the preference for the ene-then-yne mechanism is and these discrepancies seem to arise from the different bulk of the considered models. The higher the bulk included in the model, the lower the preference for the ene-then-yne route is. Moreover, *endo*/*exo* selectivity was not addressed in these studies.

In this context, we decided to perform a theoretical study on the RCEYM reaction of 1-allyloxy-2-propyne, using a model of the second-generation Grubbs–Hoveyda complex as precatalyst.[26] Special attention was paid to determining the most favorable mechanism: ene-then-yne or yne-then-ene. Note that 1-allyloxy-2-propyne is a simplified model of 1-allyloxy-1,1-diphenyl-2-propyne, the enyne used by one of us to evaluate the catalytic capability of a series of silica-supported Grubbs–Hoveyda complexes.[27,28] The advantage of this simplified model is that it enables us to determine the intrinsic reactivity of the two unsaturated groups of the molecule without including the effects of potential substituents. Finally, we are also interested in understanding why the *endo* product is usually not observed when five- or six-membered rings are formed.

## Computational Details

The second-generation Grubbs–Hoveyda catalyst was represented by the same model as used in our previous work.[29] It contains the actual bulk of the catalyst with the exception of the *i*PrO chelating group, which was replaced by an EtO group (**1** in Scheme 3). The reactive enyne is modelled by 1-allyloxy-2-propyne (**2** in Scheme 3), and thus the potential products of the reaction are 3-vinyl-2,5-dihydrofuran (**3**) and 3-methylene-3,6-dihydro-2*H*-pyran (**4**).

Calculations were performed with the B3LYP[30] hybrid density functional as implemented in the Gaussian 03 package.[31] The optimized geometries were obtained by using the quasi-relativistic effective core pseudo-potentials (RECP) of the Stuttgart group[32] and the associated basis sets augmented with a polarization function[33] for Ru and a 6-31G(d,p)[34] basis set for all other atoms (BSA). The nature of all computed intermediates and transition structures was verified by vibrational analysis. Energetics are obtained from single-point calculations at the BSA optimized geometries, with a larger 6-31++G(d,p) basis including diffuse functions for C, N, O, H and Cl (BSB).[35] The gas-phase thermal corrections were evaluated at 298.15 K and 1 atm by using BSA, as implemented in Gaussian 03.[31] These conditions are close to those used in the experiments that inspired the present work[28] and quite common in metathesis reactions.[12,16] Solvent effects were included by performing single-point calculations at the gas-phase optimized geometries with the C-PCM continu-

  

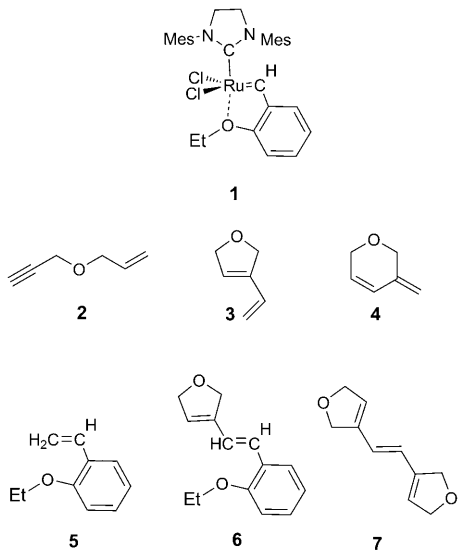


Scheme 3. Schematic representation of initial precatalyst **1**, reactant **2** and all species that are potentially formed during the catalytic process.

um model[36] and a cavity generated by using the United Atom Topological Model on radii optimized at the HF/6-31G(d) level of theory.[37] $CH_2Cl_2$, which is often used experimentally, was chosen as solvent. Moreover, dispersion forces were taken into account by including Grimme's empirical correction $D$[38] at the optimized geometry, as calculated with MOLDRAW program[39] (scaling factor 1.05). Unless otherwise indicated, all energetics reported here ($G_{gp}+\Delta G_{solv}+D$) are based on gas-phase Gibbs energies $G_{gp}$ plus solvation free energies $\Delta G_{solv}$ and Grimme's correction for dispersion forces $D$. Gas-phase free energies were obtained by combining potential energies computed with the largest BSB basis sets and the thermal corrections computed with the smallest BSA basis. Energy profiles based on $G_{gp}+\Delta G_{solv}$ (no dispersion included) and $E_{BSB}+\Delta G_{solv}$ (neither dispersion nor entropic contribution included) can be found in Figures S1–S14 in the Supporting Information.

## Results

First, we discuss the general aspects of the ene-then-yne and yne-then-ene mechanisms. Since the same elementary steps are identified for all ene-then-yne and yne-then-ene pathways reported here, we first describe these two pathways in detail. Afterwards, we present the energetics associated with 1) precatalyst activation and 2) the productive propagating catalytic cycles. The nomenclature used in the text is constructed from a number and two letters. The capital letter indicates whether a specific intermediate is involved in an ene-then-yne (**E**) process or in an yne-then-ene (**Y**) process, and the lower case letter identifies the nature of the process (**a** = precatalyst activation, **b** = propagating cycle, and **c** = active-species interconversion). Transition structures are indicated by adding **TS** before the names of the two interconnected intermediates. The words ***exo*** and ***endo*** are used to state the relative orientation between the incoming alkyne fragment and the active species.

For the precatalyst activation process, the two pathways, ene-then-yne and yne-then-ene, were considered (Scheme 4a and b). This leads to the formation of three different carbenes that can be considered as propagating species, **5Ea**, **7Ea** and **8Ya** (Scheme 4a and b). The first two belong to the ene-then-yne route and the third belongs to the yne-then-ene pathways. On the ene-then-yne pathway, we have taken **7Ea** as the propagating alkylidene since it is the most stable. Moreover, with this choice generation of the propagating carbene always implies reaction of one ene and one yne group, the only difference being the order in which they react (Scheme 4a and b). Once formed, these two active carbenes can enter the propagating catalytic cycle and proceed through an ene-then-yne mechanism from **7Ea** (Scheme 4c) or an yne-then-ene mechanism from **8Ya** (Scheme 4d and e) by coordination of a new enyne molecule. Moreover, in the yne-then-ene process starting from **8Ya**, two different alkyne approaches can be envisaged: *exo* and *endo*. Finally, one can not exclude the yne-then-ene reaction from **7Ea** and the ene-then-yne reaction from **8Ya** (Scheme 4f and g). These two processes are not productive but they allow interconversion between the two propagating species. All of these possibilities were considered in the present work, as summarized in Scheme 4. Note that *endo*-yne-then-ene precatalyst activation was not considered, because it leads to the same reacting species as the *exo*-yne-then-ene process and seems less likely to occur due to the steric hindrance between the Hoveyda ligand and the reacting enyne.[40]

**General mechanistic considerations**: All here-considered processes of precatalyst activation, propagating carbene interconversion and the propagating catalytic cycles correspond to an RCEYM reaction of 1-allyloxy-2-propyne, the only difference between them being the nature of the starting carbene and the order in which the unsaturated groups of the reagent react. Thus all processes share common steps with very similar intermediates and transition structures.

The ene-then-yne route consists of 1) an intermolecular cross-metathesis process between the initial carbene and the alkene moiety of **2** and 2) subsequent intramolecular ring-closing alkyne reorganization (Scheme 5). The cross-metathesis process takes place by the so-called Chauvin mechanism,[2,41] which according to our calculations involves four steps: olefin coordination, cycloaddition, cycloreversion and olefin decoordination. Alkene coordination leads to olefin complex **2E** with Ru···$C_{ene}$ distances ranging between 2.43 and 2.50 Å. This process requires rotation about the metal–carbene double bond by about 90°. This rotation is known to have a low energy barrier[29] but it implies enough electronic reorganization to avoid barrierless olefin coordination. In the transition structure for olefin coordination (**$TS_{1E-2E}$**) the carbene fragment is rotated by about 30° and the incoming olefin is still far from the metal centre. The Ru···$C_{ene}$ distance varies between 3.08 and 3.23 Å. To our knowledge, this transition structure has never been reported before by any of the already published computational studies on Ru-based enyne metathesis[21,24,25] or simply alkene metathesis.[22,42] This is probably because the potential-

  

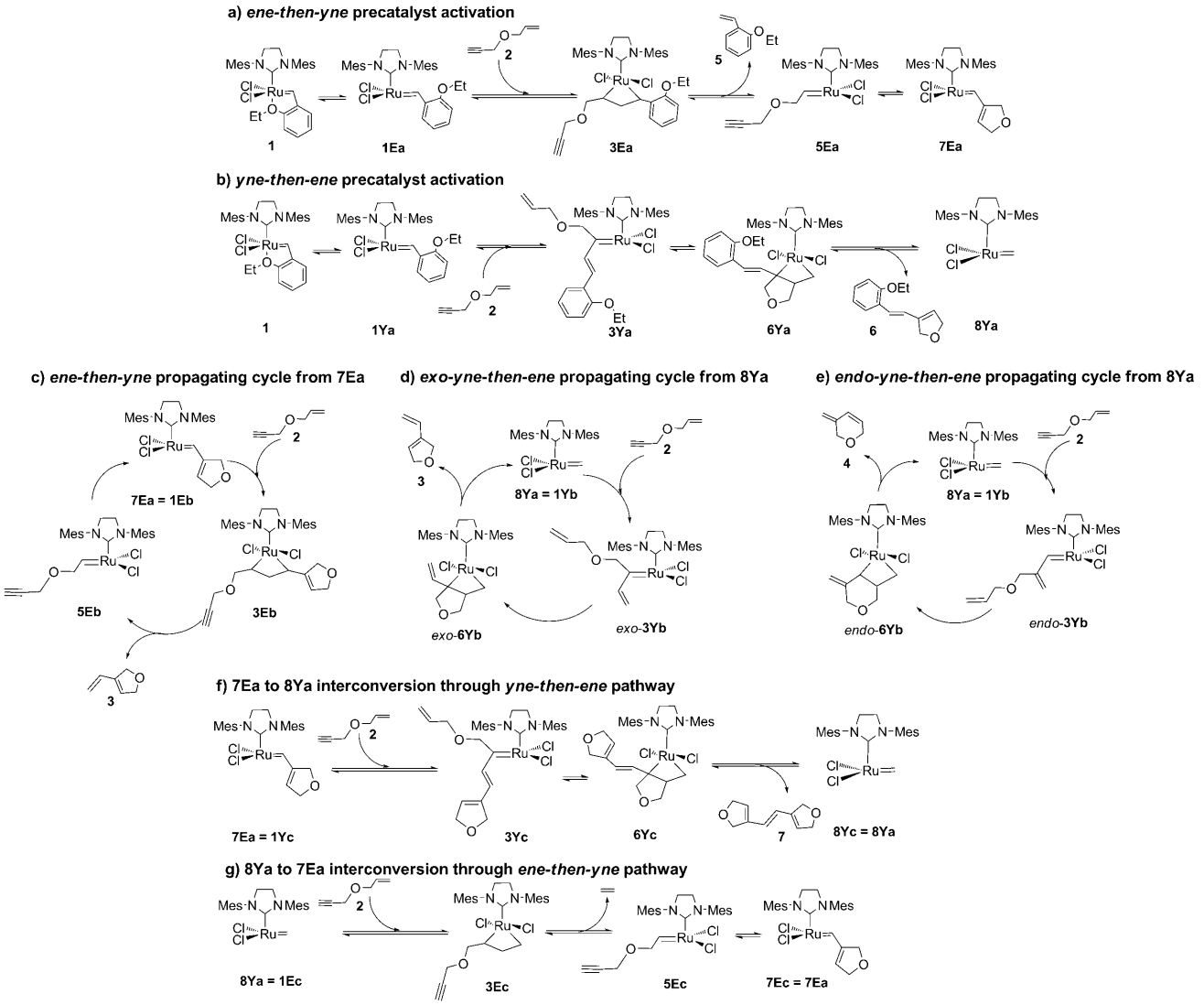


Scheme 4.

energy surface around this transition structure is very flat. Nevertheless, after considering solvation effects, the entropic contribution and the dispersive forces, the barrier height becomes of the same order of magnitude and usually even higher than that associated with all other transition structures involved in the whole mechanism. Thus, although the entropic contribution may be somewhat overestimated, this transition structure is expected to have implications for the reaction rate (see below). Note that $E_{BSB}+\Delta G_{solv}$ energies already predict that the transition structure for olefin coordination/decoordination lies higher in energy than those of the Chauvin mechanism (see Supporting Information). Equivalent coordination/decoordination transition structures have been well identified in Schrock-type catalysts,[43] and rationalization of the factors decreasing their barriers has significantly helped in the development of new and more efficient catalysts.[44]

After formation of **2E**, cycloaddition takes place leading to metallacyclobutane **3E**. All of the metallacyclobutane intermediates reported here share the same geometrical features:[29,45] trigonal-bipyramidal coordination around the metal center with the two chlorine ligands occupying the apical positions, a flat metallacycle with two long $C_\alpha$–$C_\beta$ and $C_{carbene}$–$C_\beta$ bonds and a surprisingly short Ru···$C_\beta$ distance (see Scheme 6a for labelling). The cycloaddition transition structures (**$TS_{2E-3E}$**) already have a trigonal bipyramidal like coordination around the ruthenium centre with a relatively short Ru···$C_\alpha$ distance (between 2.14 and 2.15 Å) and a $C_{carbene}$···$C_\beta$ bond which is being formed (between 2.15 and 2.16 Å). Metallacyclobutane cycloreversion leads to a new olefin complex (**4E**) in which the carbene group and the olefin have exchanged their substituents with respect to **2E**. Finally, decoordination of the new olefin leads to formation of carbene **5E**. The transition structure for this process

  

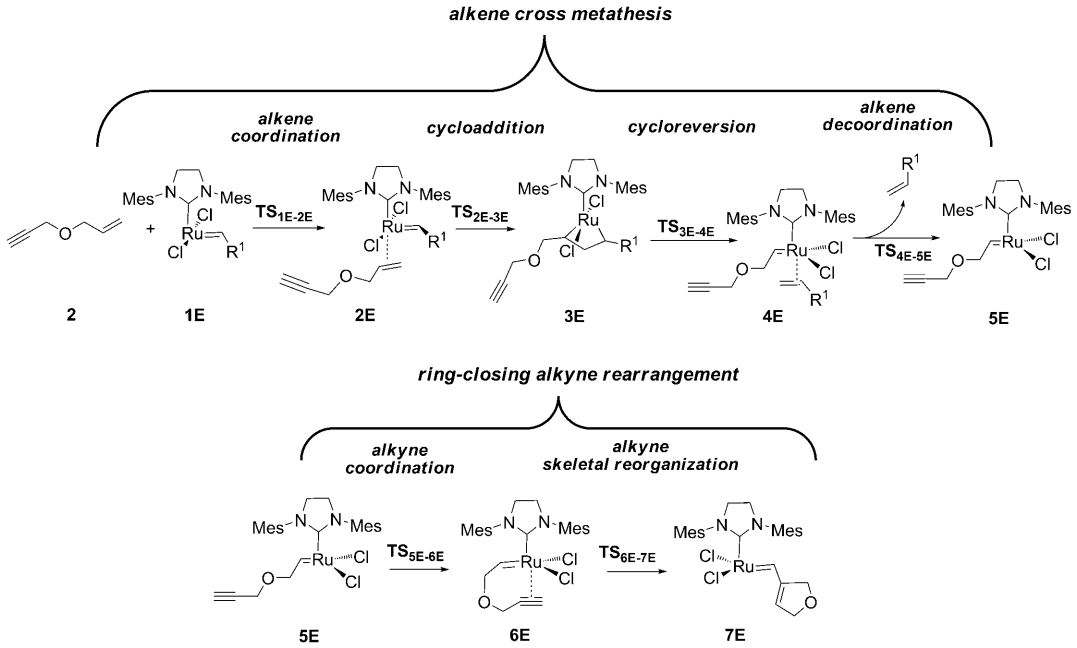


Scheme 5.

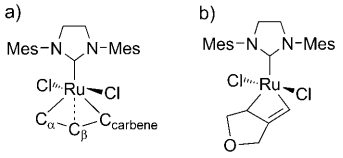


Scheme 6. Schematic representation of the general features of the metallacyclobutane and metallacyclobutene intermediates.

(**TS$_{4E-5E}$**) shares similar geometrical features to that of olefin coordination (**TS$_{1E-2E}$**).

The intramolecular alkyne metathesis process (lower part of Scheme 5) occurs in two steps: 1) alkyne coordination and 2) alkyne skeletal reorganization. The alkyne fragment coordinates to the metal centre to generate alkyne complex **6E** through the **TS$_{5E-6E}$** transition structure. This process involves simultaneous rotation about the C1−C2 single bond and the metal carbene bond and coordination of the alkyne moiety (see Scheme 7a for labelling). Noteworthily, although the C1−C2 and metal-carbene rotations are known to have low energy barriers, the associated reorganizations prevent the alkyne coordination from being barrierless. The alkyne adduct has Ru···C$_{yne}$ distances of 2.28 and 2.34 Å, which are shorter than those of the olefin adducts and suggests a slightly stronger local Ru–alkyne interaction. The skeletal alkyne reorganization from **6E** takes place in one step, as previously highlighted by Lippstreu and Straub,[24] since the hypothetical metallacyclobutene (see Scheme 6b) is not a minimum of the potential-energy surface. It spontaneously reorganizes to generate conjugated carbene **7E**. Finally, coordination of a second enyne through the alkene group starts a new ene-then-yne cycle.

In the yne-then-ene mechanism, two different routes can be distinguished depending on the relative orientation between the reactant and the Ru=C fragment of the catalyst (*exo* or *endo*). Nevertheless, the orientation of the reactant does not alter the number and nature of the elementary steps. It is for this reason that generalities are only presented for the *exo* route and particularities of the *endo* approach are discussed in the Energetics section. The *exo*-yne-then-ene route differs from the ene-then-yne route in the order in which the unsaturated groups react (see Scheme 8 for further details). This means that the intermolecular process corresponds to the alkyne skeletal reorganization (upper part of Scheme 8) and the intramolecular process to alkene ring-closing metathesis (lower part of Scheme 8). This slightly modifies the geometrical features of the intermediates and transition structures described above; the main differences are observed in the alkyne and alkene coordination steps.

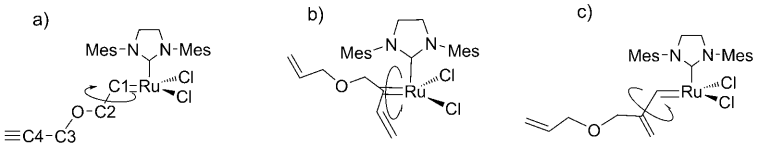


Scheme 7. Rotational processes of the carbene fragment involved in intramolecular coordination of the unsaturated fragment. a) C1−C2 rotation for intramolecular coordination of the alkyne fragment. b) Carbene rotation for intramolecular coordination of the alkene fragment in *exo* orientation. c) C1−C2 rotation for intramolecular coordination of the alkene fragment in *endo* orientation.

  

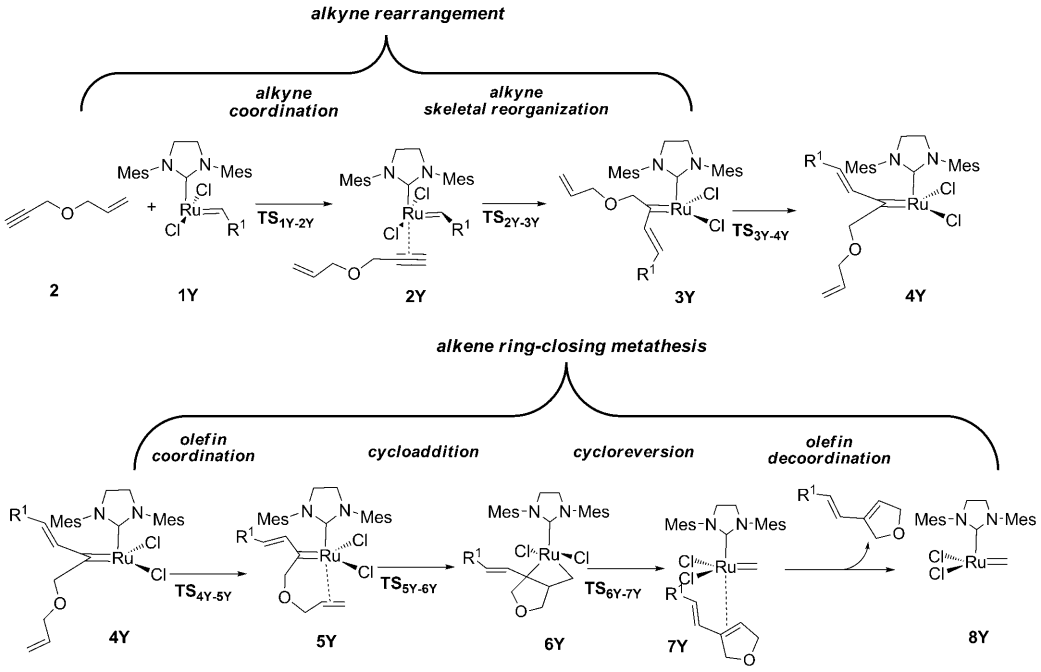


Scheme 8.

Intermolecular alkyne coordination leads to formation of alkyne complex **2Y**, which has Ru···$C_{yne}$ distances ranging between 2.10 and 2.16 Å. These distances are about 0.30 Å shorter than those computed for olefin complexes **2E** (Scheme 5) and suggest a stronger local interaction between the alkyne and the metal centre, in agreement with previous results of Lippstreu and Straub[24] and Cavallo et al.[21] The transition structure of the alkyne coordination was located for the precatalyst activation process and the propagating alkylidene interconversion. In both cases, the incoming alkyne is still far from the metal centre. Comparison between $\mathbf{TS_{5E-6E}}$ and $\mathbf{TS_{1Y-2Y}}$ reveals that the Ru···$C_{yne}$ distances are shorter for $\mathbf{TS_{1Y-2Y}}$ (3.47 and 3.10 Å) and this is associated with a larger rotation about the metal carbene bond with respect to the initial complex **1Y**.

Alkene coordination to **3Y** requires two steps (Scheme 8): 1) reorganization of the carbene fragment ($\mathbf{TS_{3Y-4Y}}$) to place the alkene moiety and the metal centre close enough for subsequent coordination and 2) alkene coordination itself ($\mathbf{TS_{4Y-5Y}}$). According to the geometry of the $\mathbf{TS_{3Y-4Y}}$ transition structure, carbene reorganization is not assisted by any stabilization arising from an interaction between the carbene substituents and the ruthenium centre, since all carbene substituents are located far from the metal centre (see Scheme 7b and c for a description of the reorganization processes taking place). Intramolecular alkene coordination itself ($\mathbf{TS_{4Y-5Y}}$) has a transition structure very similar to that of intermolecular alkene coordination ($\mathbf{TS_{1E-2E}}$) with Ru···$C_{ene}$ distances that are still long (>3 Å) and a partially rotated carbene ligand.

## Energetics

*Propagating carbene generation*: Precatalyst activation through the ene-then-yne and yne-then-ene pathways leads to **7Ea** and **8Ya**, respectively (Scheme 4a and b). Figure 1 shows the alkoxyl dissociation from the initial Grubbs–Hoveyda precatalyst, Figure 2 the Gibbs energy profile for generation of carbene **7Ea** starting from **1Ea** via the ene-then-yne route and Figure 3 the equivalent Gibbs energy profile for generation of carbene **8Ya** via the yne-then-ene pathway. All optimized intermediates and transition structures can be found in Figures S15 and S16 in the Supporting Information together with their Cartesian coordinates and absolute energies. Formation of **7Ea** and **8Ya** is exergonic, with reaction Gibbs energies of −26.7 and −23.6 kcal mol$^{-1}$, respectively. Nevertheless, the two processes must overcome several transition structures whose Gibbs energies are high above the initial Grubbs–Hoveyda precatalyst **1** (>20 kcal mol$^{-1}$). This is mainly because precatalyst activation requires endergonic Hoveyda ligand dissociation prior to entering the RCEYM mechanism described above (Figure 1).[46] This process is common to the ene-then-yne and yne-then-ene pathways, and leads to the formation of **1Ea**, a carbene with a seesaw geometry and a vacant site *trans* to the *N*-heterocyclic carbene (NHC) ligand. The reaction Gibbs energy is +11.7 kcal mol$^{-1}$ and it implies overcoming a free-energy barrier of 18.7 kcal mol$^{-1}$.[47]

From **1Ea**, the coordination of **2** through the alkene fragment enters the ene-then-yne propagating carbene generation route (Scheme 4a and Figure 2), while coordination of **2** through the alkyne fragment leads to the yne-then-ene route (Scheme 4b and Figure 3). The Gibbs energy barriers

  

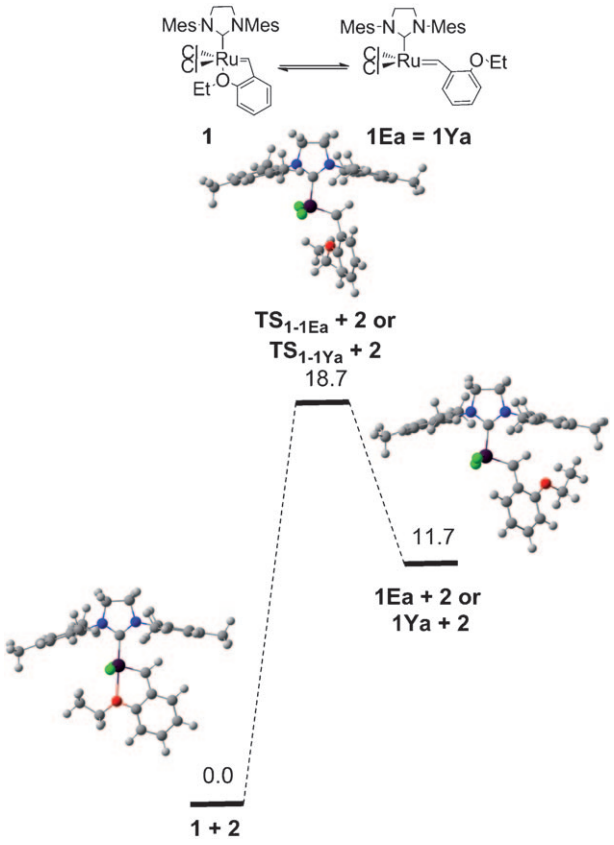


Figure 1. Gibbs energy profile (based on $G_{gp}+\Delta G_{solv}+D$ in kcal mol$^{-1}$) for alkoxyl dissociation of the Hoveyda ligand.

of the individual steps associated with precatalyst activation by the ene-then-yne route, once alkoxyl dissociation of the Hoveyda ligand has taken place, range from 3.6 to 10.5 kcal mol$^{-1}$ (Figure 2). The lowest barriers correspond to intramolecular alkyne coordination and to those of the so-called Chauvin mechanism (cycloaddition and cycloreversion), that is, the metathesis process itself is extremely easy. The highest barriers are associated with olefin coordination ($\Delta G^{\neq}=$ 9.7 kcal mol$^{-1}$), olefin decoordination ($\Delta G^{\neq}=10.5$ kcal mol$^{-1}$) and alkyne skeletal reorganization ($\Delta G^{\neq}=10.0$ kcal mol$^{-1}$).

The Gibbs energy barriers associated with precatalyst activation through the yne-then-ene route, when alkoxyl dissociation of the Hoveyda ligand has already taken place (Figure 3), range from 2.8 to 10.4 kcal mol$^{-1}$. Interestingly, although in this case the Gibbs energy barriers for cycloaddition and cycloreversion are somewhat higher (8.0 and 8.3 kcal mol$^{-1}$), probably due to the greater rigidity associated with the fact that the process is intramolecular, the highest free-energy barriers correspond to intermolecular alkyne coordination (10.4 kcal mol$^{-1}$) and subsequent alkyne skeletal reorganization (9.0 kcal mol$^{-1}$).

The preference for one process or the other depends on the energetics of the whole reaction and, for the yne-then-ene process, once alkyne reorganization has occurred, all intermediates and transition structures are much lower in energy than the initial reagents. This is in contrast to the ene-then-yne route, for which only the last step is really exergonic. Due to the complexity of establishing a rigorous equation for the reaction rate, one can assume, in a simplified analysis, that the reaction rate depends on the energy difference between the most stable intermediate and the highest-energy transition structure, similar to the concept of energy span ($\delta E=$ energy difference between the rate-determining intermediate and the rate-determining transition structure in a catalytic cycle), as defined in the work of Kozuch and Shaik for catalytic cycles.[48] Using this approximation, one notices that the highest Gibbs energy difference in the ene-then-yne precatalyst activation route is 25.4 kcal mol$^{-1}$, which corresponds to the Gibbs energy difference between the catalyst precursor (**1**+**2**) and the transition structure for decoordination of the alkene moiety ($\mathbf{TS_{4Ea-5Ea}}$). On the other hand, the free-energy difference between the most stable intermediate (**1**+**2**) and the highest transition structure ($\mathbf{TS_{2Ya-3Ya}}$) in the yne-then-ene mechanism is 24.0 kcal mol$^{-1}$. Overall, the two processes (ene-then-yne and yne-then-ene) have very similar free-energy requirements ($\Delta\Delta G^{\neq}=1.4$ kcal mol$^{-1}$) and thus formation of both **7Ea** and **8Ya** propagating carbenes is expected to be feasible if a unsubstituted enyne is used as reacting species.[49]

Once **7Ea** and **8Ya** are formed, they can react with any of the olefins present in the medium, that is, with **2**, **5** or **6** of Scheme 3. Reaction with **5** and **6** would lead to the regeneration of the initial catalyst, and thus these reactions do not lead to a productive route. Reaction of **2** in appropriate orientation with **7Ea** or **8Ya** corresponds to the RCEYM propagating cycle and the obtained results are discussed below. Finally, with the aim of being exhaustive, we also explored the possibility that **2** reacts with **7Ea** by an yne-then-ene mechanism and that **2** reacts with **8Ya** through an ene-then-yne pathway.

*Propagating catalytic cycle and interconversion of active carbene species*: Since formation of neither **7Ea** nor **8Ya** can be excluded from calculations (see above), we considered both species as propagating carbenes. This leads to three possible catalytic cycles: the ene-then-yne process starting from **7Ea**, the *exo*-yne-then-ene process starting from **8Ya** and the *endo*-yne-then-ene pathway starting from **8Ya**. We also explored the possibility that **7Ea** reacts with **2** through an yne-then-ene pathway and that carbene complex **8Ya** reacts with **2** through an ene-then-yne route. These two processes are not productive since they lead to the formation of ethene in the former case and **7** (Scheme 3) in the latter but they interconvert the two propagating species and, consequently, this may influence the relative amount of the two propagating species. The Gibbs energy profiles of all these processes are shown in Figures 4–7 and Figure S17 of the Supporting Information and include the optimized geometries of the most significant intermediates. All other structures associated with these five processes, as well as their absolute energies and Cartesian coordinates, can be found in Figures S18–S22 in the Supporting Information.

  

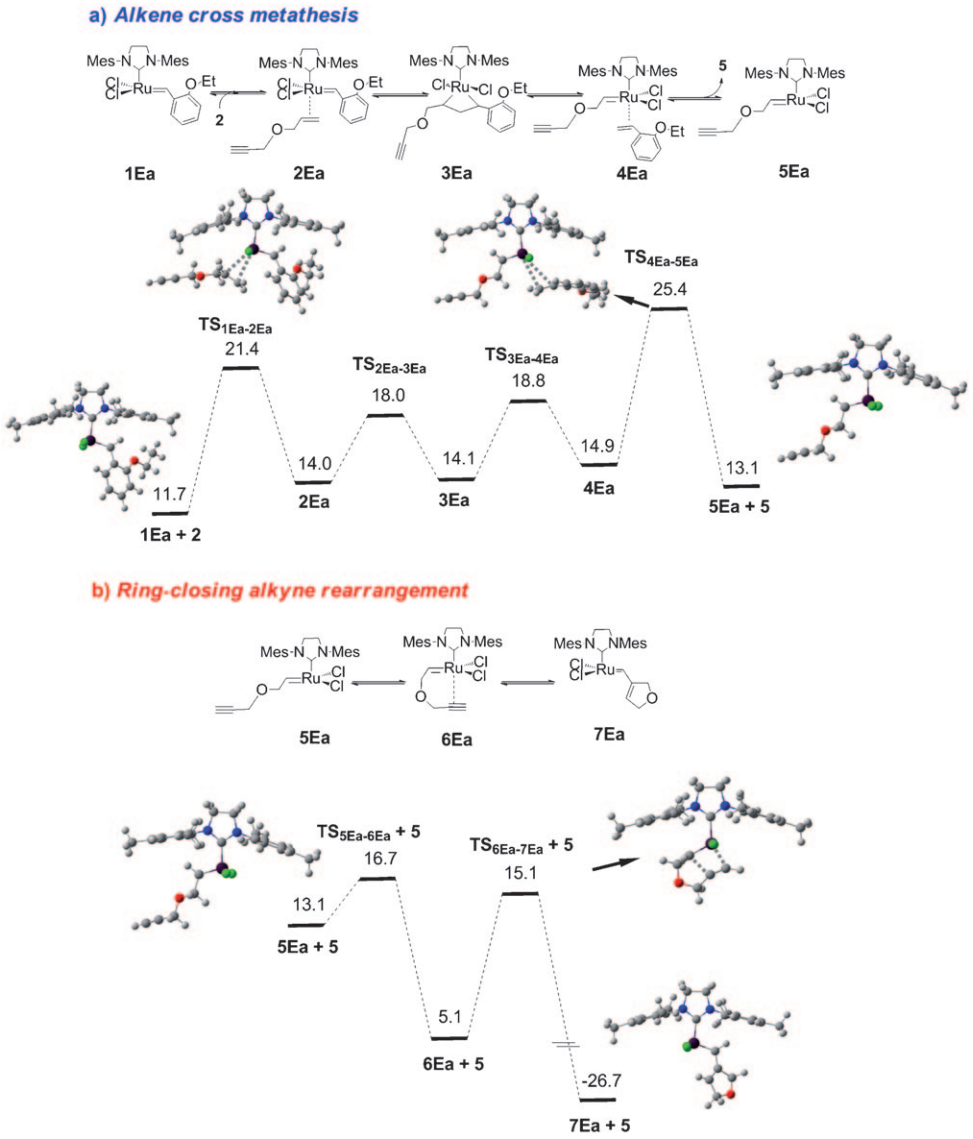


Figure 2. Gibbs energy profile (based on $G_{gp}+\Delta G_{solv}+D$ in kcal mol$^{-1}$) for generation of active carbene **7Ea** from **1Ea**. This process implies reaction of the alkene and alkyne groups of **2** through an ene-then-yne pathway. The origin of Gibbs energies is fixed to the initial precatalyst (**1**+**2**).

The ene-then-yne RCEYM process from **7Ea**+**2** to **7Ea**+**3** is very exergonic ($\Delta G=-35.4$ kcal mol$^{-1}$), but as in the case of precatalyst activation the exergonicity arises from the final alkyne reorganization step (Figure 4). In fact, intermolecular alkene metathesis is endergonic by 4.4 kcal mol$^{-1}$ and the key metallacyclobutane intermediate lies 2.4 kcal mol$^{-1}$ above the reactants. All Gibbs energy barriers resemble those of precatalyst activation, excluding the initial alkoxyl dissociation at **1**. In particular, the alkene coordination and alkene decoordination energy barriers (**TS$_{1Eb-2Eb}$** and **TS$_{4Eb-5Eb}$**) are marginally lower than those associated with the equivalent process of precatalyst activation, **TS$_{1Ea-2Ea}$** and **TS$_{4Ea-5Ea}$** (8.6 versus 9.7 and 9.8 versus 10.5 kcal mol$^{-1}$, respectively). This is probably due to the smaller hindrance of the carbene, as reflected by the lower relative energy of olefin complex **2Eb** (Figure 4) compared with that of precatalyst activation, **2Ea** (Figure 2). In contrast, the cycloaddition and cycloreversion steps are slightly higher than those of precatalyst activation (5.6 and 5.1 kcal mol$^{-1}$ versus 4.0 and 4.7 kcal mol$^{-1}$), but they are always lower than the olefin coordination and decoordination steps. Overall, the Gibbs energy span of the catalytic cycle is small, as would be expected considering the high efficiency of this catalytic cycle. It is 14.3 kcal mol$^{-1}$ and it arises from the energy difference between the propagating carbene **7Ea**+**2** and the transition structure **TS$_{4Eb-5Eb}$** for olefin decoordination (Figure 4).

The reaction of **2** with **7Ea** through an yne-then-ene pathway leading to the propagating carbene **8Ya** and **7** (see Scheme 3 for olefin definition) is also a very exergonic reaction ($\Delta G=-32.6$ kcal mol$^{-1}$) (Figure 5). As in the case of the precatalyst activation through the yne-then-ene process,

  

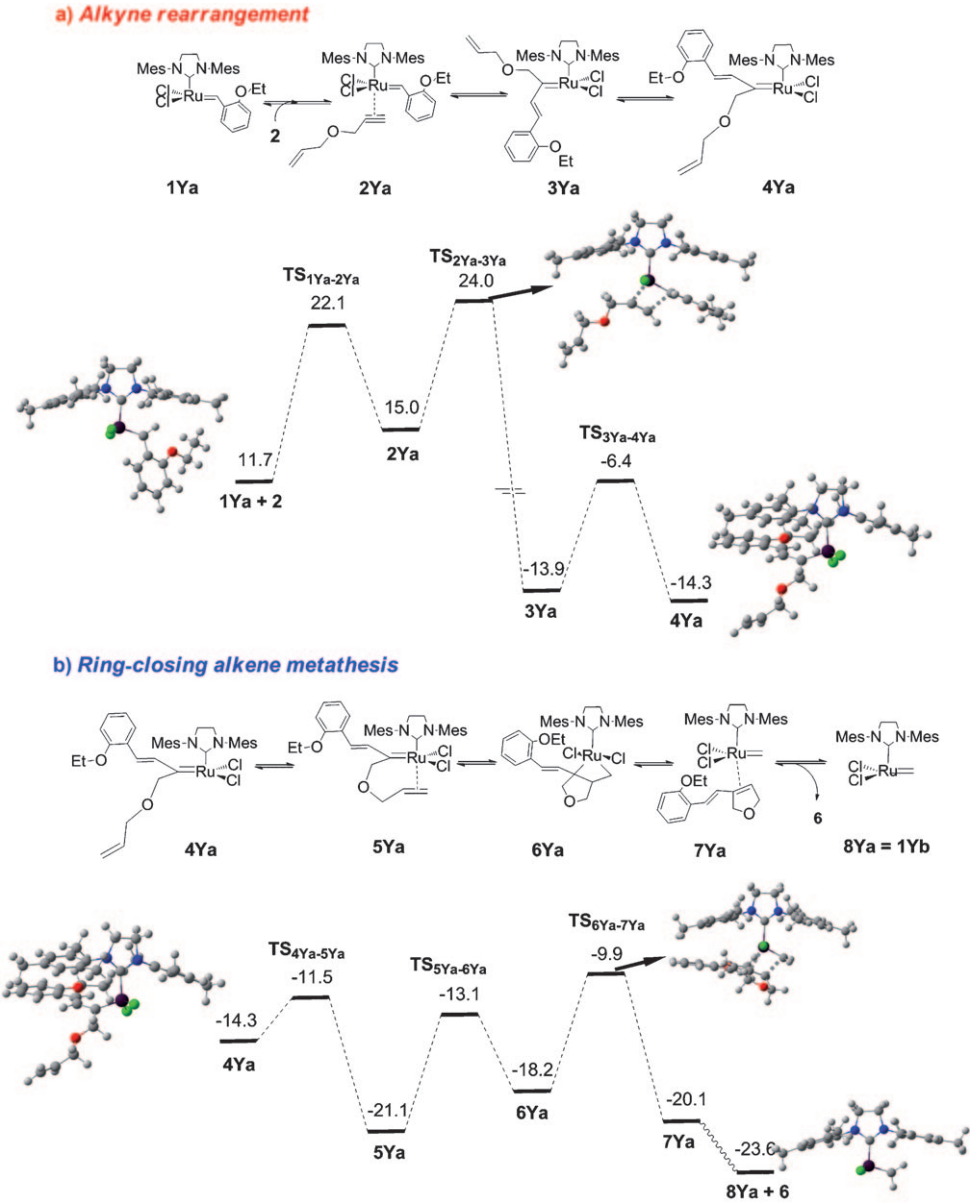


Figure 3. Gibbs energy profile (based on $G_{gp}+\Delta G_{solv}+D$ in kcal mol$^{-1}$) for the generation of active carbene **8Ya** from **1Ya**. This process implies reaction of the alkene and alkyne groups of **2** through an yne-then-ene pathway. The origin of Gibbs energies is fixed to the initial precatalyst (**1**+**2**).

the most energetically demanding steps are associated with 1) coordination of the alkyne fragment ($\mathbf{TS_{1Yc-2Yc}}$), 2) alkyne skeletal reorganization ($\mathbf{TS_{2Yc-3Yc}}$) and 3) carbene reorganization prior to alkene coordination ($\mathbf{TS_{3Yc-4Yc}}$). The corresponding energy barriers are 11.0, 9.5 and 11.4 kcal mol$^{-1}$ for $\mathbf{TS_{1Yc-2Yc}}$, $\mathbf{TS_{2Yc-3Yc}}$ and $\mathbf{TS_{3Yc-4Yc}}$, respectively. However, once alkyne skeletal reorganization has taken place, all other intermediates and transition structures are well below the reactants, which suggests that after formation of **3Yc** regeneration of the initial species is ruled out. As a consequence, the $\mathbf{TS_{3Yc-4Yc}}$ transition structure does not seem to play a very important role in determining the feasibility of this process. Overall, the Gibbs energy difference between reactants and the transition structure of highest free energy is 11.9 kcal mol$^{-1}$, which is 2.4 kcal mol$^{-1}$ smaller than the Gibbs energy span associated with the catalytic ene-then-yne process starting from **7Ea**. The differences in Gibbs energies between the two processes are small and may be influenced by the modelling strategy. Nevertheless, present calculations suggest that the two processes are likely to occur, and thus the methylidene species (**8Ya**) should become slightly more abundant during the process, in particular because the reverse reaction (**8Ya** to **7Ea**) is less likely to take place (see Figure S17 of the Supporting Information and below).

The *exo*-yne-then-ene catalytic cycle (Figure 6) also leads to formation of product **3**, and thus the overall thermodynamics is the same as that of the ene-then-yne route from

  

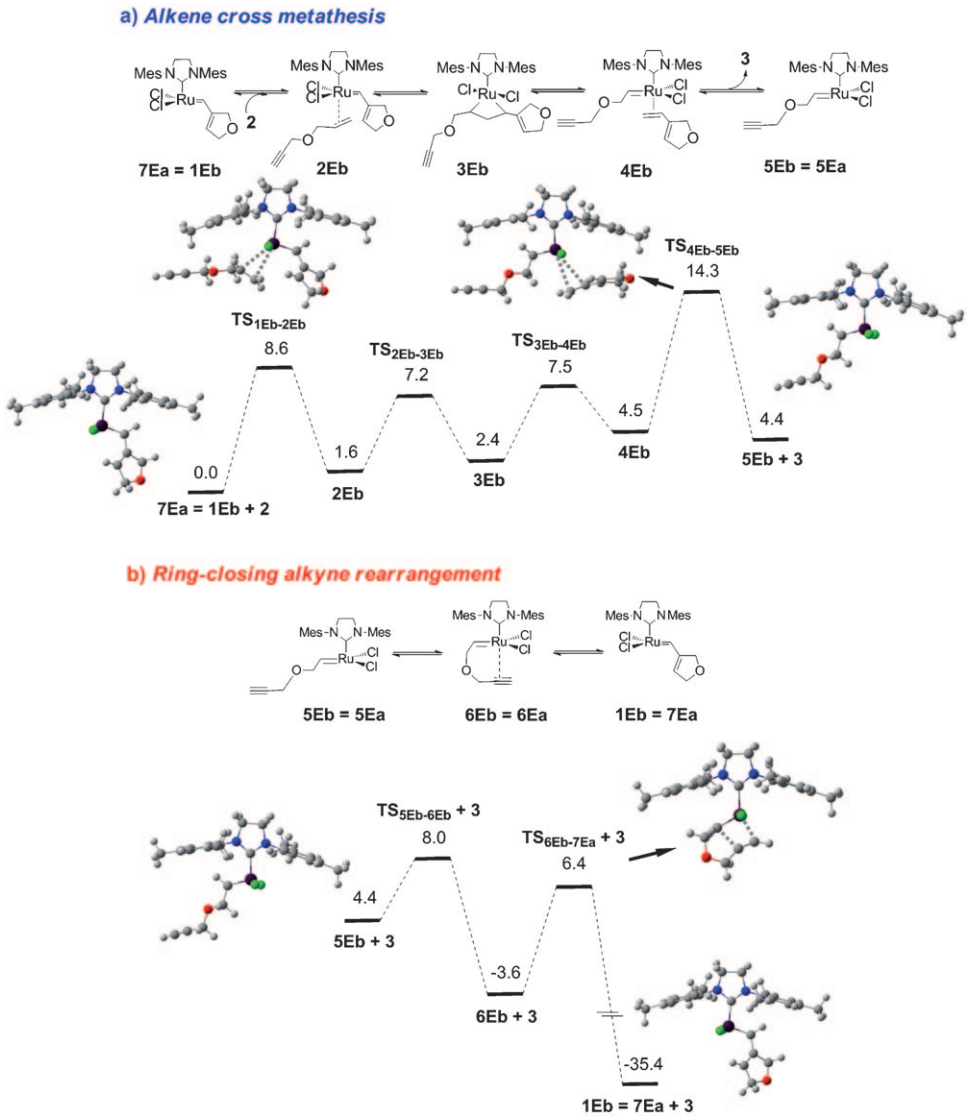


Figure 4. Gibbs energy profile (based on $G_{gp}+\Delta G_{solv}+D$ in kcal mol$^{-1}$) for the propagating catalytic cycle through the ene-then-yne pathway. Some selected optimized structures have been added.

**7Ea**. Note, however, that while in the ene-then-yne route the exergonicity arises from the last steps, in the yne-then-ene mechanism it arises from the first ones. Therefore, only the transition structures for alkyne coordination and alkyne skeletal reorganization are above the reactants. Unfortunately, we have not been able to locate any transition structure for coordination of the unsaturated fragment to **8Ya**, neither for alkyne nor for alkene coordination, and this may be related to the smaller bulk of the methylidene complex. Nevertheless, one should expect the existence of transition structures equivalent to those of the previous situations (reaction of **2** with **1Ea** or **7Ea**) at least in terms of Gibbs energies due to the entropic loss (Figures 2–5). In any case, the Gibbs energy barriers for alkene and alkyne coordination in the precatalyst activation process are similar ($\Delta G^{\ddagger}=9.7$ and 10.4 kcal mol$^{-1}$, respectively; Figures 2 and 3) and in the reaction of **2** with **7Ea** ($\Delta G^{\ddagger}=8.6$ and 11.0 kcal mol$^{-1}$; Figures 4 and 5). Therefore, we envisage that the equivalent processes involving **2** and **8Ya** would show similar barriers for alkene and alkyne coordination and probably lower than those of transition structures $\mathbf{TS_{1Ea-2Ea}}$, $\mathbf{TS_{1Eb-2Eb}}$, $\mathbf{TS_{1Ya-2Ya}}$ and $\mathbf{TS_{1Yc-2Yc}}$ ($<11$ kcal mol$^{-1}$). As a consequence, the Gibbs energy span $\delta G$ for the *exo*-yne-then-ene route starting from **8Ya** arises from the difference between the ***exo*-3Yb** intermediate and the ***exo*-$\mathbf{TS_{3Yb-4Yb}}$** transition structure. This span is slightly smaller than that of the ene-then-yne catalytic cycle [$\delta G=11.9$ kcal mol$^{-1}$ (Figure 6) versus 14.3 kcal mol$^{-1}$ (Figure 4)], and thus calculations suggest that the yne-then-ene route is expected to be marginally faster.

On the other hand, the *endo*-yne-then-ene route (Figure 7) generates diene **4** (Scheme 3), which has a six-membered ring. The overall process is thermodynamically preferred to that generating **3** by 4.6 kcal mol$^{-1}$ ($\Delta G=-40.0$ versus $-35.4$ kcal mol$^{-1}$). Nevertheless, the higher exergonicity does not correlate with lower individual Gibbs energy barriers, and in fact, at first glance, one would say that the Gibbs energy profile largely resembles that of the *exo*-yne-then-ene route. In detail, one can observe that carbene reorganization to allow intramolecular alkene coordination (***endo*-$\mathbf{TS_{3Yb-4Yb}}$**) is energetically easier in the *endo* pathway than in the *exo* one. This preferences arises from the fact that carbene reorganization only requires rotation about the C1–C2 single bond (Scheme 7c) instead of about the Ru=C bond. In contrast, the alkyne skeletal reorganization (***endo*-$\mathbf{TS_{2Yb-3Yb}}$**) is more energetically demanding ($\Delta G^{\ddagger}=9.0$ kcal mol$^{-1}$ versus 6.8 kcal mol$^{-1}$ for *endo* and *exo* routes, respectively). Overall, the resulting energy span ($\delta G=10.0$ kcal mol$^{-1}$), which arises from the Gibbs energy difference between the **1Yb+2** propagating carbene and the ***endo*-$\mathbf{TS_{2Yb-3Yb}}$** transition structure, is 1.9 kcal mol$^{-1}$ lower than that computed for the *exo*-yne-then-ene route. However, alkyne skeletal reorganization is an irreversible process ($\Delta G<-25$ kcal mol$^{-1}$). Therefore, since both pathways (*exo*- and *endo*-yne-then-ene) involve the same reacting species, the preference for one process or

  

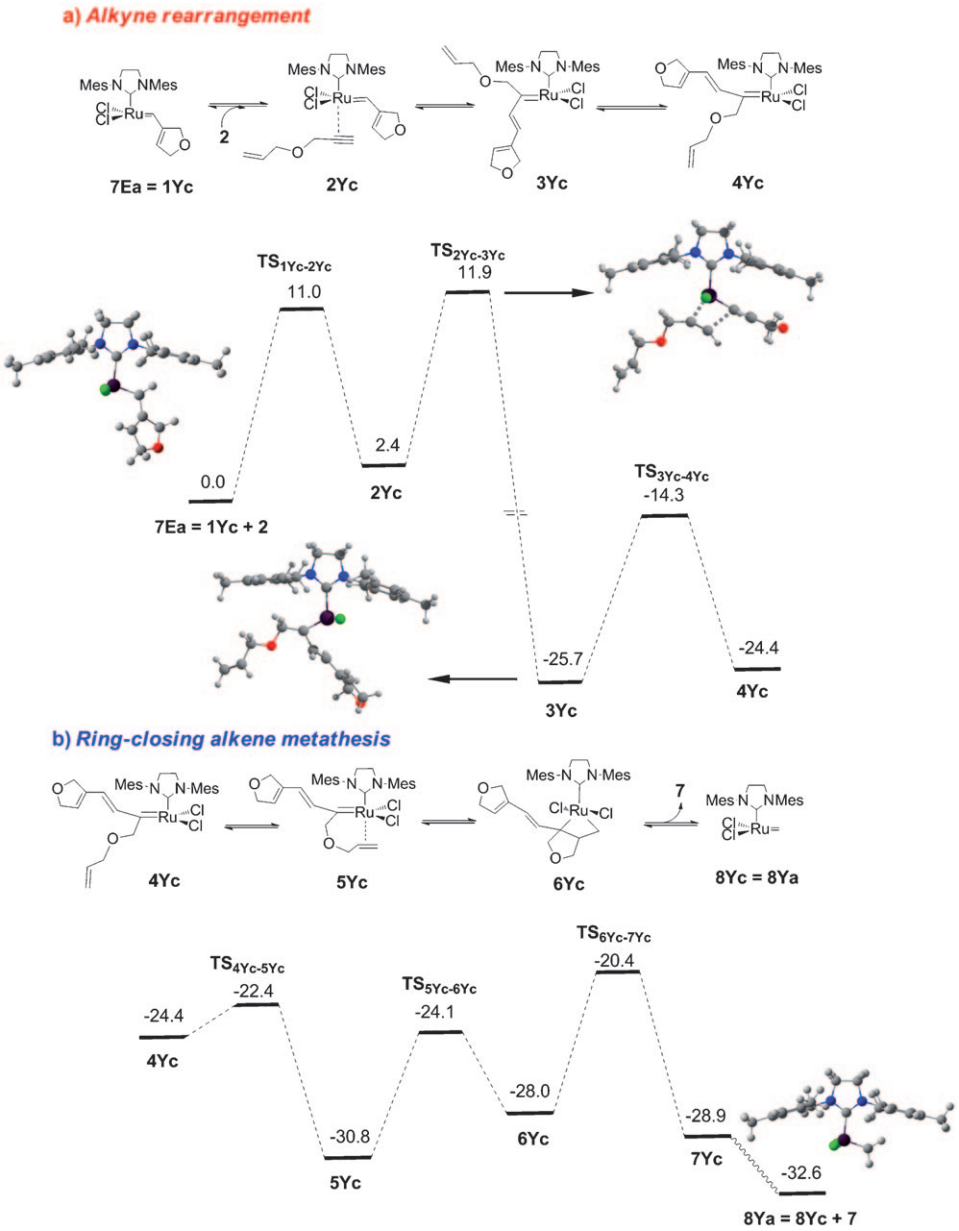


Figure 5. Gibbs energy profile (based on $G_{gp}+\Delta G_{solv}+D$ in kcal mol$^{-1}$) for the **7-Ea** to **8-Ya** interconversion through an yne-then-ene pathway.

the other would mainly arise from the Gibbs energy barrier required for alkyne skeletal reorganization in each case (the irreversible step). This reorganization requires overcoming energy barriers of 6.7 kcal mol$^{-1}$ in the *exo* approach and 10.0 kcal mol$^{-1}$ in the *endo* orientation. Overall, the former is kinetically preferred, and this energy difference may explain why the *exo* species is usually observed as the major or, more frequently, the only product.

We also considered the possibility that **8Ya** reacts with **2** by an ene-then-yne mechanism. Figures S17 and S22 in the Supporting Information show the Gibbs energy profile ($G_{gp}+\Delta G_{solv}+$D) associated with this process and the optimized structures, respectively. Although we could not find the transition structure associated with alkene coordination, formation of the metallacyclobutane intermediate appears to be easy and exergonic ($\Delta G=-7.2$ kcal mol$^{-1}$), in agreement with the observation of poorly substituted metallacyclobutane species.[50] Nevertheless, and due to the high stability of metallacyclobutane intermediate **3Ec**, the Gibbs energy barrier for generation of carbene **5Ec** and subsequent alkyne skeletal reorganization is significantly high ($\Delta G^{\neq}=16.3$ kcal mol$^{-1}$), especially when compared to those computed for the propagating processes. As a consequence, interconversion of **8Ya** and **7Ea** seems less likely to occur and thus, although interconversion is not ruled out, **8Ya** seems to mainly proceed by an yne-then-ene pathway.

## Discussion

Scheme 9 summarizes the computed Gibbs energy differences defining the process efficiency of all studied pathways (energy spans[48] for catalytic cycles and the energy difference between the lowest intermediate and highest transition structure for the others). As expected, precatalyst activation, either by the ene-then-yne or yne-then-ene route, shows larger Gibbs energy differences between the extreme stationary points ($\Delta G^{\neq}$ are 25.4 and 24.0 kcal mol$^{-1}$, respectively). These values are more than 10 kcal mol$^{-1}$ larger than the energy spans associated with the propagating catalytic cycles, and this is mainly due to the energetic cost of alkoxyl decoordination ($\Delta G=11.7$ kcal mol$^{-1}$). Consequently, the catalytic process seems to be largely influenced by precatalyst activation.

The reaction rate for the activation process through the ene-then-yne route is determined by the Gibbs energy difference between the Grubbs–Hoveyda precatalyst and decoordination of the alkene fragment. This implies two key factors: 1) the loss of stability due to decoordination of the chelating Hoveyda ligand and 2) the free-energy cost for coordination/decoordination of the alkene fragment. The first

  

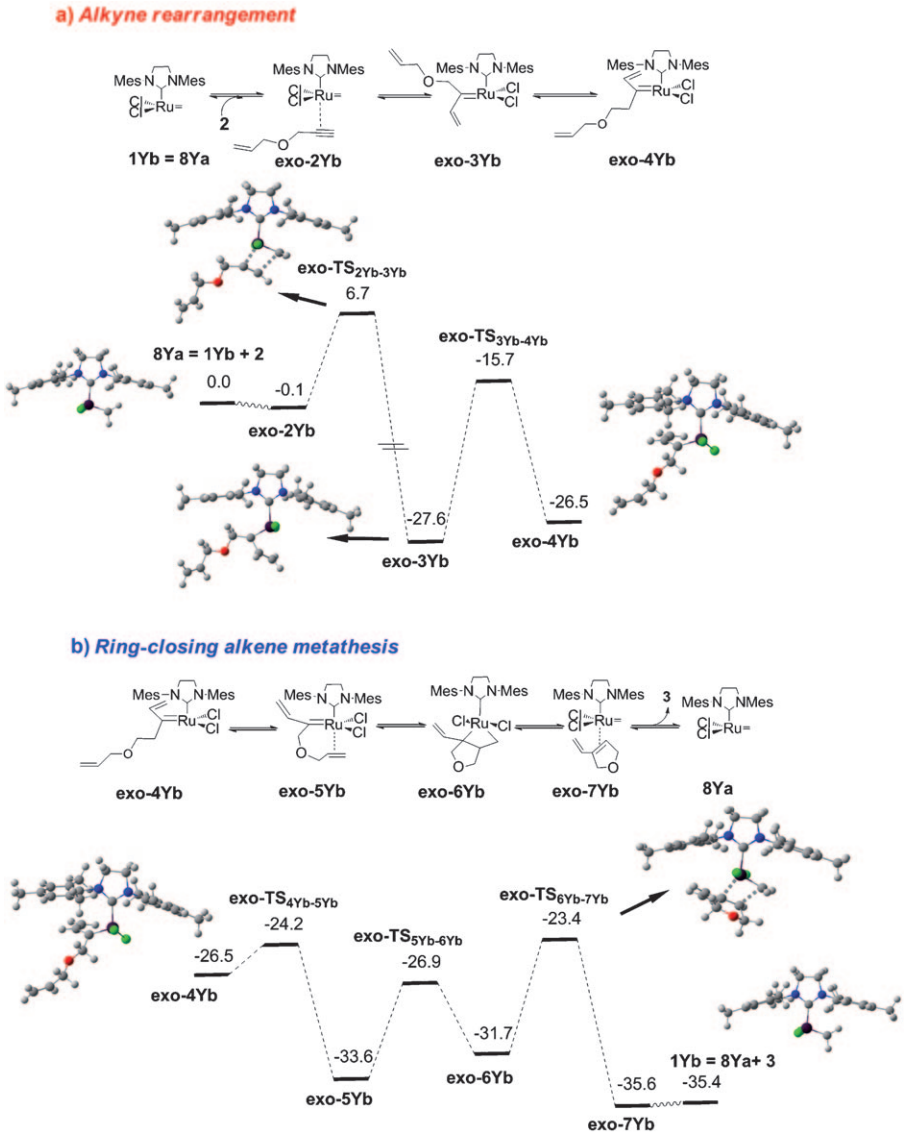


Figure 6. Gibbs energy profile (based on $G_{gp}+\Delta G_{solv}+D$ in kcal mol$^{-1}$) for the propagating catalytic cycle through the *exo*-yne-then-ene pathway.

factor was highlighted and its electronic origin recently discussed by some of us.[29] The second factor has been much less discussed. Nevertheless, alkoxyl dissociation alone does not allow rationalization of all existing experimental data. In our opinion, the interplay of the two factors allows an understanding of all evidence: 1) the dependence of the catalytic activity on the nature of the substituents of the Hoveyda ligand,[5,51] 2) the negative activation entropies[52] and 3) the dependence of the activation rate on the concentration of the unsaturated reactant.[53] The first evidence is explained by the role of benzene substituents in the loss of precatalyst stability by alkoxyl dissociation, and the other two by the fact that the rate-determining transition structures involve the metal complex and the reacting unsaturated species. We are currently carrying out additional calculations to rationalize the role of all these effects. In any case, the present calculations suggest that from a mechanistic point of view the dissociative pathway may apply as established previously for first-generation Grubbs catalysts, but the rate-determining step may correspond in these cases to the coordination/decoordination steps of the unsaturated fragment. Furthermore, since none of the here-computed Gibbs energy barriers traditionally associated with the alkene metathesis process (cycloaddition and cycloreversion) are higher in free energy than those of the alkene coordination or decoordination steps, these steps should be taken into account when discussing Ru-based olefin metathesis processes, even though the limitations on the modelling here may overestimate its importance.

On the other hand, the reaction rate for the activation through the yne-then-ene route is determined by the Gibbs energy difference between the precatalyst and alkyne skeletal reorganization. Thus, although coordination of the alkyne fragment requires overcoming a free-energy barrier similar to that of alkene coordination on the ene-then-yne pathway, the transition structure for alkyne reorganization lies at even higher Gibbs energies.

Regarding the preference for the ene-then-yne or the yne-then-ene route, the computed Gibbs energy differences between the two routes are beyond the accuracy of the modelling. Moreover, the key transition structures of the ene-then-yne and yne-then-ene routes are different in nature, and this makes the analysis even more difficult. As a consequence, although our calculations suggest a small preference for the yne-then-ene route, the data calculated here suggest that neither of the two routes should be excluded, that is, both the ene-then-yne and the yne-then-ene pathways seem to be plausible. The preference for the *endo* or *exo* reactant orientation in the yne-then-ene route seems to be mainly controlled by the free-energy barrier prior to irreversible alkyne reorganization. Thus, the *exo*-yne-then-ene is suggested to be more likely than the *endo*-yne-then-ene one because it has a lower Gibbs energy barrier to alkyne skeletal reorganization

  

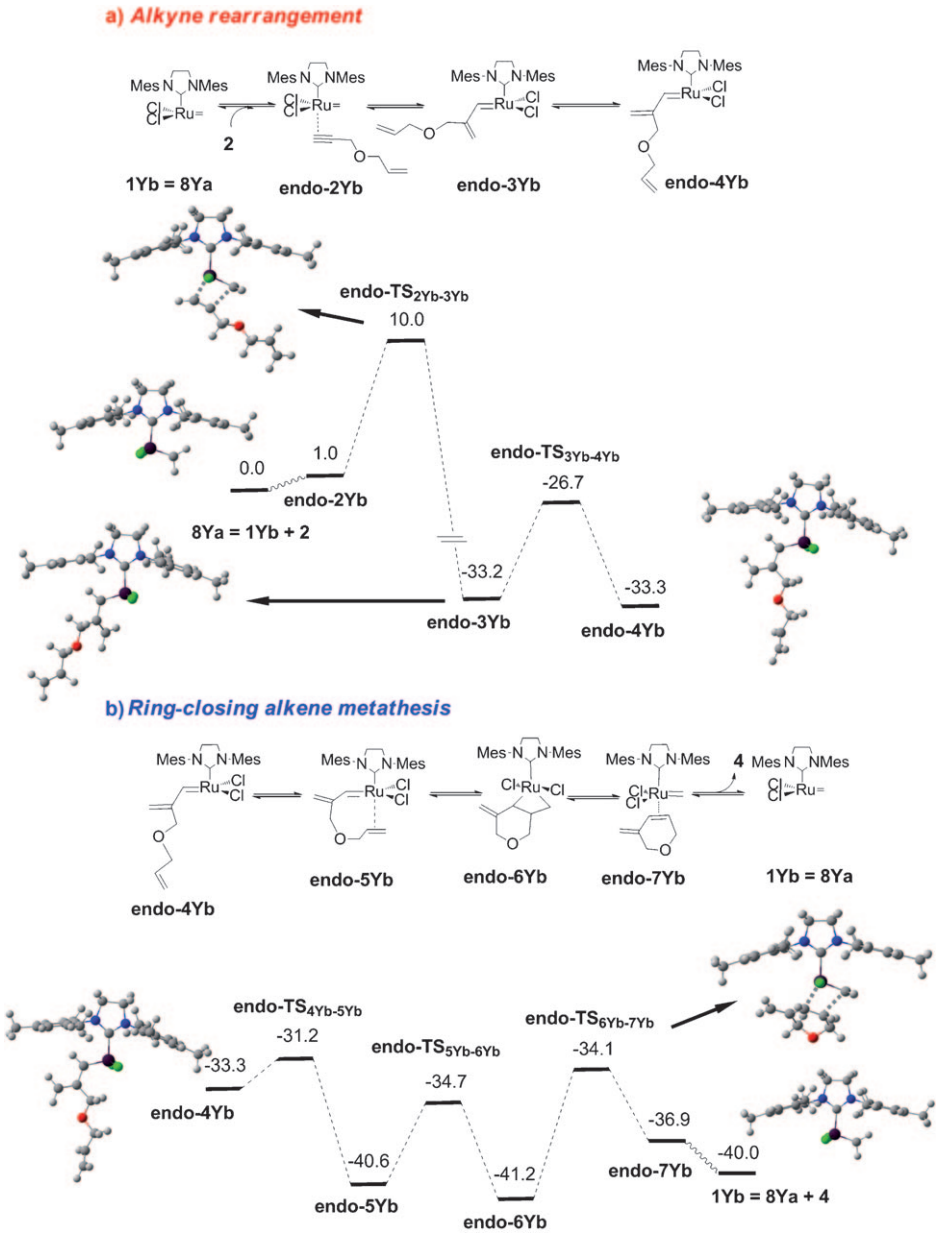


Figure 7. Gibbs energy profile (based on $G_{gp}+\Delta G_{solv}+D$ in kcal mol$^{-1}$) for the propagating catalytic cycle through the *endo*-yne-then-ene pathway.

(6.8 versus 9.0 kcal mol$^{-1}$). Overall, our results indicate a slight preference for formation of the *exo* product through the yne-then-ene route. Nevertheless, taking into account the limitations of our modelling, we conclude that none of the pathways studied here—ene-then-yne, *exo*-yne-then-ene and *endo*-yne-then-ene—is really ruled out.

All these considerations seem to explain, at least in part, the major controversy concerning the mechanism of enyne metathesis. All reagents used to determine the mechanism have substituents either close to the alkene or close to the alkyne fragment, and this may favour one or the other mechanism.[15,16] In contrast, the slight preference for the *exo* product seems to be in sharp contradiction with experimental evidence, since up to now, most of the RCEYM reactions performed with Ru-based catalyst have led to unique formation of the *exo* product,[17,18,54] and we have only been able to find very scarce examples in which the *endo* product is formed in appreciable amounts.[17,18,20] However, experiments are always performed with substituted enynes, and these substituents may again play a crucial role in *exo* versus *endo* selectivity.

In summary, calculations indicate no intrinsic preference for any of the potential routes (ene-then-yne or yne-then-ene) of RCEYM, and this suggests that the preferred pathway and product formation are dependent on reactant, probably catalyst (not studied here) and reaction conditions. Accurate analysis of the role of the enyne substituents is needed, but this is beyond the scope of the present work. We are currently performing calculations to analyze which substituents may favour the *exo* or *endo* product.

## Conclusions

In summary, the following conclusions can be drawn from the present results:

1) We have reported for the first time the existence of transition structures for coordination and decoordination of unsaturated fragments, the potential energy barriers of which are small. Nevertheless, after considering solvation effects, the entropic contribution and the dispersion forces, the resulting free-energy barriers become competitive with the highest ones of the global mechanism. Moreover, the existence of this initial step in the precatalyst activation process allows rationalization of the experimentally determined energetics, as well as the observed dependence between substrate concentration and the activation rate.
2) Cycloaddition and cycloreversion steps are always extremely easy, the highest computed Gibbs energy barrier being 8.3 kcal mol$^{-1}$. This suggests that the preference for

  

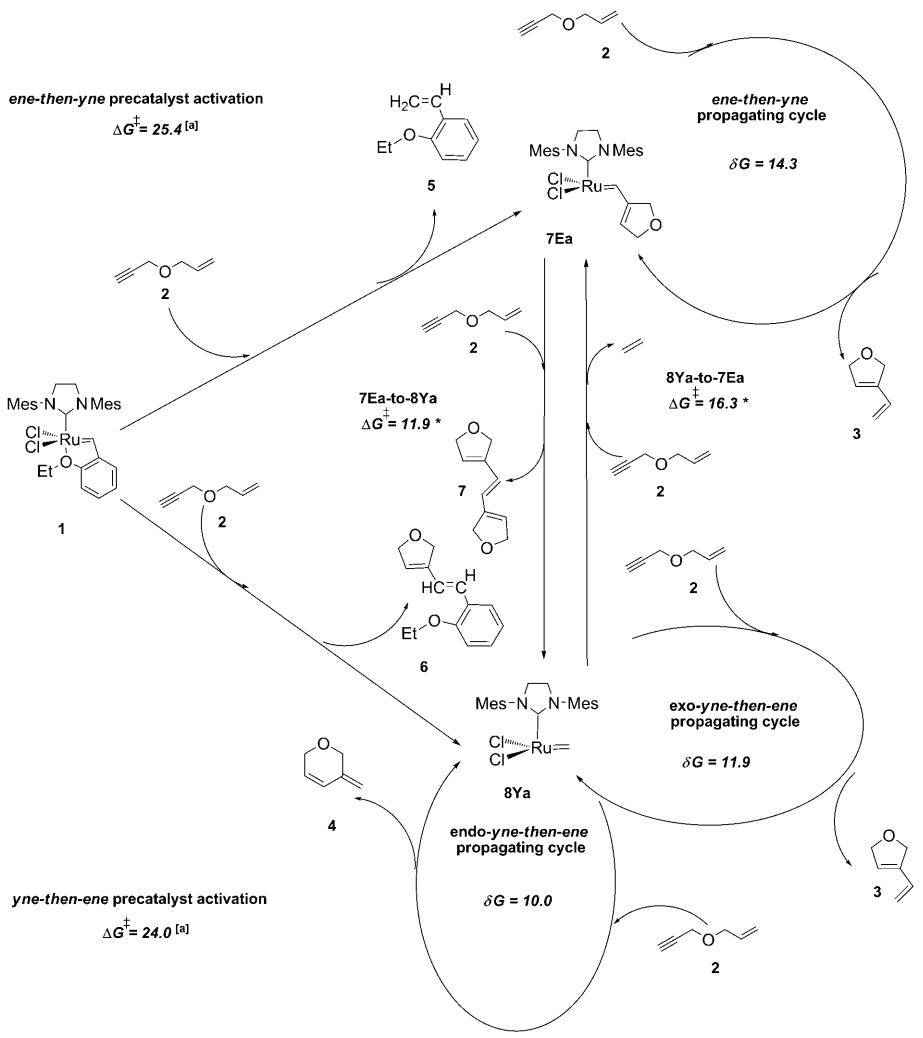


Scheme 9. [a] $\Delta G^{\ddagger}$ refers to the energy difference between the lowest in energy intermediate and the highest transition state in each process. Energies in kcal mol$^{-1}$.

one or the other route (ene-then-yne or yne-then-ene) is to a large extent controlled by alkyne skeletal reorganization and the alkene-fragment coordination and decoordination steps. Nevertheless, although the rate-determining species are different for the two pathways, the associated Gibbs energy barriers are very similar when an unsubstituted enyne is used as reactant. As a consequence, both the ene-then-yne and yne-then-ene mechanisms seem to be potentially operative in RCEYM processes, and the operative mechanism is likely dependent on the reaction conditions.

3) Formation of the *endo* product through a RCEYM process with Ru-based catalyst is not ruled out a priori. Thus, substrates disfavouring the initial coordination/decoordination of the alkene fragment (key steps of the ene-then-yne route) could lead to formation of some amounts of the *endo* product.

## Acknowledgements

We acknowledge financial support from MICINN (projects CTQ2008-06381/BQU and CTQ2009-07881/BQU), Consolider Ingenio 2010 (Project CSD2007-00006), Generalitat de Catalunya (Projects SGR2009-01441, SGR2009-638). F.N.Z. wishes to thank to Universitat Autònoma de Barcelona for his PIF grant and X.S.M. also thanks the Spanish MEC/MICINN for his Ramón y Cajal fellowship.

[1] N. Calderon, H. Y. Chen, K. W. Scott, *Tetrahedron Lett.* **1967**, *8*, 3327–3330.
[2] Y. Chauvin, *Angew. Chem.* **2006**, *118*, 3824–3831; *Angew. Chem. Int. Ed.* **2006**, *45*, 3740–3747.
[3] R. H. Grubbs, *Angew. Chem.* **2006**, *118*, 3845–3850; *Angew. Chem. Int. Ed.* **2006**, *45*, 3760–3765; R. R. Schrock, *Angew. Chem.* **2006**, *118*, 3832–3844; *Angew. Chem. Int. Ed.* **2006**, *45*, 3748–3759.
[4] a) D. Astruc, *New J. Chem.* **2005**, *29*, 42–56; b) M. R. Buchmeiser, *Chem. Rev.* **2000**, *100*, 1565–1604; c) A. Fürstner, *Angew. Chem.* **2000**, *112*, 3140–3172; *Angew. Chem. Int. Ed.* **2000**, *39*, 3012–3043; d) J. C. Mol, *J. Mol. Catal. A* **2004**, *213*, 39–45; e) C. Copéret, *Dalton Trans.* **2007**, 5498–5504; f) M. Schuster, S. Blechert, *Angew. Chem.* **1997**, *109*, 2124–2144; *Angew. Chem. Int. Ed. Engl.* **1997**, *36*, 2036–2056.
[5] M. Bieniek, A. Michrowska, D. L. Usanov, K. Grela, *Chem. Eur. J.* **2008**, *14*, 806–818.
[6] E. C. Hansen, D. Lee, *Acc. Chem. Res.* **2006**, *39*, 509–519.
[7] a) P. H. Deshmukh, S. Blechert, *Dalton Trans.* **2007**, 2479–2491; b) S. T. Diver, *Coord. Chem. Rev.* **2007**, *251*, 671–701; c) K. J. Ivin, J. C. Mol, *Olefin Metathesis and metathesis polymerization*. 2nd ed., Academic Press, San Diego, **1997**, p. 496.
[8] S. T. Diver, A. J. Giessert, *Chem. Rev.* **2004**, *104*, 1317–1382.
[9] H. Villar, M. Frings, C. Bolm, *Chem. Soc. Rev.* **2007**, *36*, 55–66.
[10] T. J. Katz, T. M. Sivavec, *J. Am. Chem. Soc.* **1985**, *107*, 737–738.
[11] A. Kinoshita, M. Mori, *Synlett* **1994**, 1020–1022.
[12] M. Mori, N. Sakakibara, A. Kinoshita, *J. Org. Chem.* **1998**, *63*, 6082–6083.
[13] R. Stragies, M. Schuster, S. Blechert, *Angew. Chem.* **1997**, *109*, 2628–2630; *Angew. Chem. Int. Ed. Engl.* **1997**, *36*, 2518–2520.
[14] a) H. Y. Lee, B. G. Kim, M. L. Snapper, *Org. Lett.* **2003**, *5*, 1855–1858; b) A. Nunez, A. M. Cuadro, J. Alvarez-Builla, J. J. Vaquero, *Chem. Commun.* **2006**, 2690–2692; c) M. Mori, *J. Mol. Catal. A* **2004**, *213*, 73–79; d) C. S. Poulsen, R. Madsen, *Synthesis* **2003**, 1–18.
[15] N. Dieltiens, K. Moonen, C. V. Stevens, *Chem. Eur. J.* **2007**, *13*, 203–214.
[16] G. C. Lloyd-Jones, R. G. Margue, J. G. de Vries, *Angew. Chem.* **2005**, *117*, 7608–7613; *Angew. Chem. Int. Ed.* **2005**, *44*, 7442–7447.
[17] V. Sashuk, K. Grela, *J. Mol. Catal. A* **2006**, *257*, 59–66.
[18] T. Kitamura, Y. Sato, M. Mori, *Adv. Synth. Catal.* **2002**, *344*, 678–693.

  

[19] K. H. Kim, T. Ok, K. Lee, H. S. Lee, K. T. Chang, H. Ihee, J. H. Sohn, *J. Am. Chem. Soc.* **2010**, *132*, 12027–12033.
[20] T. Kitamura, Y. Sato, M. Mori, *Chem. Commun.* **2001**, 1258–1259.
[21] H. Clavier, A. Correa, E. C. Escudero-Adan, J. Benet-Buchholz, L. Cavallo, S. P. Nolan, *Chem. Eur. J.* **2009**, *15*, 10244–10254.
[22] a) L. Cavallo, *J. Am. Chem. Soc.* **2002**, *124*, 8965–8973; b) A. Correa, L. Cavallo, *J. Am. Chem. Soc.* **2006**, *128*, 13352–13353; c) S. E. Vyboishchikov, M. Bühl, W. Thiel, *Chem. Eur. J.* **2002**, *8*, 3962–3975; d) S. E. Vyboishchikov, W. Thiel, *Chem. Eur. J.* **2005**, *11*, 3921–3935; e) C. Adlhart, P. Chen, *Helv. Chim. Acta* **2003**, *86*, 941–949.
[23] a) C. Costabile, L. Cavallo, *J. Am. Chem. Soc.* **2004**, *126*, 9592–9600; b) Y. Zhao, D. G. Truhlar, *Org. Lett.* **2007**, *9*, 1967–1970; c) D. Benitez, E. Tkatchouk, W. A. Goddard, *Chem. Commun.* **2008**, 6194–6196; d) I. C. Stewart, D. Benitez, D. J. O'Leary, E. Tkatchouk, M. W. Day, W. A. Goddard, R. H. Grubbs, *J. Am. Chem. Soc.* **2009**, *131*, 1931–1938; e) C. Adlhart, P. Chen, *J. Am. Chem. Soc.* **2004**, *126*, 3496–3510; f) C. Adlhart, P. Chen, *Angew. Chem.* **2002**, *114*, 4668–4671; *Angew. Chem. Int. Ed.* **2002**, *41*, 4484–4487; g) B. F. Straub, *Adv. Synth. Catal.* **2007**, *349*, 204–214; h) M. Jordaan, P. van Helden, C. van Sittert, H. C. M. Vosloo, *J. Mol. Catal. A* **2006**, *254*, 145–154; i) O. M. Aagaard, R. J. Meier, F. Buda, *J. Am. Chem. Soc.* **1998**, *120*, 7174–7182; j) R. J. Meier, O. M. Aagaard, F. Buda, *J. Mol. Catal. A* **2000**, *160*, 189–197; k) S. Fomine, J. V. Ortega, M. A. Tlenkopatchev, *Organometallics* **2005**, *24*, 5696–5701; l) S. Fomine, M. A. Tlenkopatchev, *Organometallics* **2007**, *26*, 4491–4497; m) S. Fomine, S. M. Vargas, M. A. Tlenkopatchev, *Organometallics* **2003**, *22*, 93–99.
[24] J. J. Lippstreu, B. F. Straub, *J. Am. Chem. Soc.* **2005**, *127*, 7444–7457.
[25] R. Garcia-Fandino, L. Castedo, J. R. Granja, D. J. Cardenas, *Dalton Trans.* **2007**, 2925–2934.
[26] a) J. S. Kingsbury, J. P. A. Harrity, P. J. Bonitatebus, A. H. Hoveyda, *J. Am. Chem. Soc.* **1999**, *121*, 791–799; b) S. B. Garber, J. S. Kingsbury, B. L. Gray, A. H. Hoveyda, *J. Am. Chem. Soc.* **2000**, *122*, 8168–8179.
[27] a) X. Elias, R. Pleixats, M. Wong Chi Man, J. J. E. Moreau, *Adv. Synth. Catal.* **2006**, *348*, 751; b) X. Elias, R. Pleixats, M. Wong Chi Man, J. J. E. Moreau, *Adv. Synth. Catal.* **2007**, *349*, 1701–1713.
[28] X. Elias, R. Pleixats, M. Wong Chi Man, *Tetrahedron* **2008**, *64*, 6770–6781.
[29] X. Solans-Monfort, R. Pleixats, M. Sodupe, *Chem. Eur. J.* **2010**, *16*, 7331–7343.
[30] a) A. D. Becke, *J. Chem. Phys.* **1993**, *98*, 5648–5652; b) C. T. Lee, W. T. Yang, R. G. Parr, *Phys. Rev. B* **1988**, *37*, 785–789.
[31] Gaussian 03, Revision B.04, M. J. Frisch, G. W. Trucks, H. B. Schlegel, G. E. Scuseria, M. A. Robb, J. R. Cheeseman, J. A. Montgomery, Jr., T. Vreven, K. N. Kudin, J. C. Burant, J. M. Millam, S. S. Iyengar, J. Tomasi, V. Barone, B. Mennucci, M. Cossi, G. Scalmani, N. Rega, G. A. Petersson, H. Nakatsuji, M. Hada, M. Ehara, K. Toyota, R. Fukuda, J. Hasegawa, M. Ishida, T. Nakajima, Y. Honda, O. Kitao, H. Nakai, M. Klene, X. Li, J. E. Knox, H. P. Hratchian, J. B. Cross, V. Bakken, C. Adamo, J. Jaramillo, R. Gomperts, R. E. Stratmann, O. Yazyev, A. J. Austin, R. Cammi, C. Pomelli, J. W. Ochterski, P. Y. Ayala, K. Morokuma, G. A. Voth, P. Salvador, J. J. Dannenberg, V. G. Zakrzewski, S. Dapprich, A. D. Daniels, M. C. Strain, O. Farkas, D. K. Malick, A. D. Rabuck, K. Raghavachari, J. B. Foresman, J. V. Ortiz, Q. Cui, A. G. Baboul, S. Clifford, J. Cioslowski, B. B. Stefanov, G. Liu, A. Liashenko, P. Piskorz, I. Komaromi, R. L. Martin, D. J. Fox, T. Keith, M. A. Al-Laham, C. Y. Peng, A. Nanayakkara, M. Challacombe, P. M. W. Gill, B. Johnson, W. Chen, M. W. Wong, C. Gonzalez, J. A. Pople, Gaussian, Inc., Wallingford, CT, **2004**.
[32] W. Küchle, M. Dolg, H. Stoll, H. Preuss, *Mol. Phys.* **1991**, *74*, 1245–1263.
[33] A. W. Ehlers, M. Böhme, S. Dapprich, A. Gobbi, A. Höllwarth, V. Jonas, K. F. Köhler, R. Stegmann, A. Veldkamp, G. Frenking, *Chem. Phys. Lett.* **1993**, *208*, 111–114.
[34] a) M. M. Francl, W. J. Pietro, W. J. Hehre, J. S. Binkley, M. S. Gordon, D. J. Defrees, J. A. Pople, *J. Chem. Phys.* **1982**, *77*, 3654–3665; b) W. J. Hehre, R. Ditchfield, J. A. Pople, *J. Chem. Phys.* **1972**, *56*, 2257–2261.
[35] P. C. Hariharan, J. A. Pople, *Theor. Chim. Acta* **1973**, *28*, 213–222.
[36] a) M. Cossi, N. Rega, G. Scalmani, V. Barone, *J. Comput. Chem.* **2003**, *24*, 669–681; b) V. Barone, M. Cossi, *J. Phys. Chem. A* **1998**, *102*, 1995–2001; c) S. Miertus, E. Scrocco, J. Tomasi, *Chem. Phys.* **1981**, *55*, 117–129.
[37] V. Barone, M. Cossi, J. Tomasi, *J. Chem. Phys.* **1997**, *107*, 3210–3221.
[38] S. Grimme, *J. Comput. Chem.* **2004**, *25*, 1463–1473; S. Grimme, *J. Comput. Chem.* **2006**, *27*, 1787–1799.
[39] P. Ugliengo, D. Viterbo, G. Chiari, *Z. Kristallogr.* **1993**, *207*, 9.
[40] The transition structure for alkyne skeletal reorganization with *endo* approach ***endo*-$TS_{2Ya-3Ya}$** is 2.8 kcal mol$^{-1}$ higher in free energy than the equivalent ***exo*-$TS_{2Ya-3Ya}$**.
[41] J. L. Hérisson, Y. Chauvin, *Makromol. Chem.* **1971**, *141*, 161–176.
[42] a) C. Adlhart, C. Hinderling, H. Baumann, P. Chen, *J. Am. Chem. Soc.* **2000**, *122*, 8204–8214; b) A. Fürstner, O. R. Thiel, L. Ackermann, H. J. Schanz, S. P. Nolan, *J. Org. Chem.* **2000**, *65*, 2204–2207.
[43] a) A. Poater, X. Solans-Monfort, E. Clot, C. Copéret, O. Eisenstein, *J. Am. Chem. Soc.* **2007**, *129*, 8207–8216; b) X. Solans-Monfort, E. Clot, C. Copéret, O. Eisenstein, *J. Am. Chem. Soc.* **2005**, *127*, 14015–14025.
[44] a) F. Blanc, R. Berthoud, A. Salameh, J. M. Basset, C. Copéret, R. Singh, R. R. Schrock, *J. Am. Chem. Soc.* **2007**, *129*, 8434–8435; b) R. Singh, R. R. Schrock, P. Muller, A. H. Hoveyda, *J. Am. Chem. Soc.* **2007**, *129*, 12654–12655; c) S. J. Malcolmson, S. J. Meek, E. S. Sattely, R. R. Schrock, A. H. Hoveyda, *Nature* **2008**, *456*, 933–937.
[45] a) C. H. Suresh, M. H. Baik, *Dalton Trans.* **2005**, 2982–2984; b) C. H. Suresh, N. Koga, *Organometallics* **2004**, *23*, 76–80.
[46] All efforts to locate an associative transition structure lead to transition structures that are more than 30 kcal mol$^{-1}$ above the initial precursor.
[47] The reported value here is slightly different from that given in reference [29], due to slightly different methods of evaluating solvent effects.
[48] a) S. Kozuch, C. Amatore, A. Jutand, S. Shaik, *Organometallics* **2005**, *24*, 2319–2330; b) S. Kozuch, S. Shaik, *J. Am. Chem. Soc.* **2006**, *128*, 3355–3365; c) S. Kozuch, S. Shaik, *J. Phys. Chem. A* **2008**, *112*, 6032–6041.
[49] As mentioned above, the *endo*-yne-then-ene route seems unlikely due to the steric repulsion that would exist between the reacting carbene and the Hoveyda ligand.
[50] a) E. F. van der Eide, W. E. Piers, *Nat. Chem.* **2010**, *2*, 571–576; b) E. F. van der Eide, P. E. Romero, W. E. Piers, *J. Am. Chem. Soc.* **2008**, *130*, 4485–4491.
[51] a) A. Michrowska, R. Bujok, S. Harutyunyan, V. Sashuk, G. Dolgonos, K. Grela, *J. Am. Chem. Soc.* **2004**, *126*, 9318–9325; b) M. Zaja, S. J. Connon, A. M. Dunne, M. Rivard, N. Buschmann, J. Jiricek, S. Blechert, *Tetrahedron* **2003**, *59*, 6545–6558.
[52] G. C. Vougioukalakis, R. H. Grubbs, *Chem. Eur. J.* **2008**, *14*, 7545–7556.
[53] a) T. Vorfalt, K. J. Wannowius, H. Plenio, *Angew. Chem.* **2010**, *122*, 5665–5668; *Angew. Chem. Int. Ed.* **2010**, *49*, 5533–5536; b) M. Gatti, L. Vieille-Petit, X. J. Luan, R. Mariz, E. Drinkel, A. Linden, R. Dorta, *J. Am. Chem. Soc.* **2009**, *131*, 9498–9499.
[54] Y. J. Lee, R. R. Schrock, A. H. Hoveyda, *J. Am. Chem. Soc.* **2009**, *131*, 10652–10661.

Received: November 25, 2010
Published online: May 26, 2011

  